Chemically Tailoring Nanopores for Single-Molecule Sensing and Glycomics

James T. Hagan, Brian S. Sheetz, Y.M. Nuwan D.Y. Bandara, Buddini I. Karawdeniya, Melissa A. Morris, Robert B. Chevalier, and Jason R. Dwyer*

¹Department of Chemistry, University of Rhode Island, 140 Flagg Rd., Kingston, RI, 02881 ²Present address: Department of Chemistry, University of Colorado Boulder, Boulder, CO, 80309.

*jason dwyer@uri.edu

ORCID

James T. Hagan: 0000-0001-8125-8596 Brian S. Sheetz: 0000-0002-7456-9692

Y.M. Nuwan D.Y. Bandara: 0000-0003-1921-8467 Buddini I. Karawdeniya: 0000-0002-2733-5973 Melissa A. Morris: 0000-0003-3634-2195 Robert B. Chevalier: 0000-0002-2907-7090 Jason R. Dwyer: 0000-0002-2938-2888

Keywords

Nanopore; electrokinetics; single-molecule sensing; nanofluidics; silicon nitride; carbohydrate

Abstract

A nanopore can be fairly—but uncharitably—described as simply a nanofluidic channel through a thin membrane. Even this simple structural description holds utility and underpins a range of applications. Yet significant excitement for nanopore science is more readily ignited by the role of nanopores as enabling tools for biomedical science. Nanopore techniques offer single-molecule sensing without the need for chemical labelling, since in most nanopore implementations, matter is its own label through its size, charge, and chemical functionality. Nanopores have achieved considerable prominence for single-molecule DNA sequencing. The predominance of this application, though, can overshadow their established use for nanoparticle characterization and burgeoning use for protein analysis, among other application areas. Analyte scope continues to be expanded and with increasing analyte complexity, success will increasingly hinge on control over nanopore surface chemistry to tune the nanopore, itself, and to moderate analyte transport. Carbohydrates are emerging as the latest high-profile target of nanopore science. Their tremendous chemical and structural complexity means that they challenge conventional chemical analysis methods and thus present a compelling target for unique nanopore characterization capabilities. Furthermore, they offer molecular diversity for probing nanopore operation and sensing mechanisms. This article thus focuses on two roles of chemistry in nanopore science: its use to provide exquisite control over nanopore performance, and how analyte properties can place stringent demands on nanopore chemistry.

Expanding the horizons of nanopore science requires increasing consideration of the role of chemistry and increasing sophistication in the realm of chemical control over this nanoscale milieu.

Introduction

Background. "You can't patent a hole" was the legal opinion that greeted Wallace H. Coulter's idea to replace the tedious, error-prone method of counting red blood cells using a microscope and human with a method of electronically counting them as they passed through an aperture.(1) In brief, the aperture provided the sole fluid connection between two reservoirs filled with electrolyte, with each containing an electrode. A red blood cell would then displace its own volume of electrolyte upon passage through the aperture, giving rise to a signal readily detectable by electronics. The Coulter name continues to be emblazoned on modern-day instrumentation employing the principle for cell and particle analysis. Put simply, "[t]he hole that could not be patented inspired a principle that could."(1)

The aperture in these red blood cell counters had to be at least as large as the micrometer-scale red blood cells. The apertures in nanopore sensing are orders of magnitude smaller, but the field uses the same general principle of operation in the most basic implementation. Passage of molecules, complexes, and nanoscale particles—from inorganic nanoparticles to biological species such as exosomes—through such dramatically scaled-down Coulter Counting devices can deliver electronic counts of species number. It is thus tantalizing to think of nanopore sensing as having originated as the nanoscale equivalent of this method, but a different invention path inspired by the nanoscale biological channels of nature has been outlined.(2) Nevertheless, consideration of how useful and prevalent a micrometer-scale aperture—a hole!—has become in cellular and particle analysis can help in imagining ambitious horizons for nanopore sensing (Figure 1). At the same time, it can provide a tangible benchmark for understanding how much greater the challenges and complexities can be when implementing the analogous principle on the nanoscale.

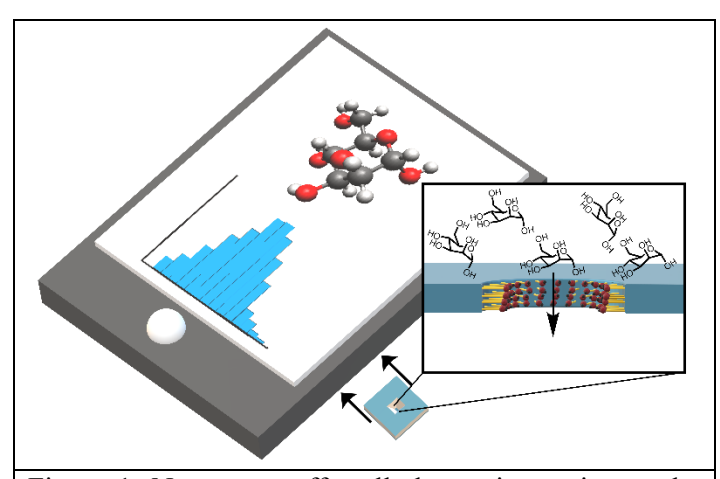


Figure 1. Nanopores offer all-electronic sensing at the level of single molecules. Selected nanopore materials ready compatibility with conventional nanofabrication workflows—and thus the potential for large-scale commercialization of nanopore-enabled consumer electronic devices. Chemistry has a powerful role to play in nanopore sensing: whether it be in broadening the breadth and complexity of the analyte scope (e.g. carbohydrates) or in tuning nanopore performance and capabilities at the molecular level. Here, a schematic nanopore-containing chip—with nanopore performance tuned by a custom molecular coating—is interfaced with a hand-held electronic device. Passage of single molecules through the nanopore can generate characteristic signals that can be analyzed in time and magnitude to reveal analyte properties and identities.

The original Coulter Counter aperture was formed with a hot needle in the cellophane wrapper of a pack of cigarettes.(1) While a flameless cigarette lighter was recently used to quickly create crude nanopore sensors(3)—practically and poetically repurposing cigarette paraphernalia for biomedical diagnostics—the task of reproducibly and controllably fabricating nanoscale apertures for nanopore sensing has been daunting and has historically required highly sophisticated measures. Transmission electron microscopes have been repurposed as nanoscale jackhammers and large-scale accelerators have been used for single heavy ion bombardment in the pursuit of nanopores in the coveted ≤10 nm diameter range. More recently—and the inspiration for the flameless lighter fabrication method—controlled dielectric breakdown (CDB) has emerged and been rigorously optimized for the reliable formation of nanopores in thin films using quite simple and cost-effective instrumentation.(4, 5) Nanopore science has thus advanced to the point where the challenge of reliably making nanopores of the desired size has been largely removed as a barrier to advancing and applying the field. Other challenges remain, however, but provide for attendant opportunities. The remainder of this article will focus on tuning nanopore performance with molecular-

level control to cope with the enormous chemical and structural complexity of carbohydrates. Analysis of this class of molecule remains one of the grand challenges of chemistry.(6-10)

Perspectives on Nanopore Tools. By suitable experimental design, nanopores offer straightforward single molecule sensing without the need for the analyte to contain intrinsic fluorophores—or to be labelled with fluorophores—as required for the more familiar single-molecule techniques relying on fluorescence. In nanopore sensing, matter is its own label, with differentiation provided by intrinsic parameters such as analyte size, charge density and polarity, and even reactivity. The same list of parameters applied to the nanopore (instead of, or in addition to, the analyte) also profoundly affects the observed signal. (At the level of a single molecule passing through a pore, it is intriguing to consider what limits—if any—sample insolubility has on nanopore sensing, and what might then be learned about solvation and ion transport). The effects of all of these parameters can be stamped on the nanopore signal in a variety of ways spanning magnitude, temporal profile including duration and frequency composition, dependence on applied voltage magnitude and polarity, and on matrix conditions. In that sense, the nanopore signal is much more than the current blockage description that is convenient for introductory descriptions of the technique. It goes beyond even recognizing that the signal can be a current enhancement (although one might not deduce this from the common appellation of this approach as "resistive pulse sensing").(11) The nanopore signal is rich with molecular-level information originating from a number of sources that can be tuned to enhance the information content that can be extracted from the signal, as well as to control the capabilities of the nanopore tool. On a grander horizon, tuning of such parameters as nanopore size and surface chemistry in conjunction with matrix composition can aid in efforts to develop nanopores as a general chemical sensor element beyond the current predominant –omics focus.(6)

While much of nanopore science focuses on its role in single-molecule sensing, other significant capabilities and application areas emerge simply by virtue of a nanopore being a *nanoscale* aperture or container. These include nanoparticle synthesis, solution filtering, providing controlled apertures between vacuum and atmosphere, and enabling fundamental studies of e.g. mass transport.(12-21) Other work has taken advantage of the size and surface chemistry of nanopores in a carbonized metal-organic framework to extract N-linked glycans from a complex matrix prior to analysis by mass spectrometry.(22) Figure 2 shows the use of (asymmetric) electroless plating to animate the use of nanopores as apertures for (here, diffusional) sample delivery. In brief, a helium ion microscope (Carl Zeiss Microscopy, LLC, Peabody, MA) was used to prepare two spatially offset 5×5 arrays of <20 nm diameter nanochannels in a 30 nm-thick SiN_x membrane (Protochips DTF-030523, Raleigh, NC). These initial pore diameters were determined by using the imaging capability of the helium ion microscope to correlate fabrication dwell times and nanochannel diameters.(23) Electroless plating involves deposition of thin metal films onto

surfaces by solution-phase redox chemistry. Briefly, for the SiN_x pores, a plasma surface pretreatment was followed by a hydrofluoric acid etch and sequential immersion in a Sn(II) surface sensitizer, an ammoniacal silver nitrate solution; and a formaldehyde-containing Au(I) solution.(24-26) The formaldehyde acts to reduce Au(I) to metallic Au. All steps here were carried out with gentle rocking in a refrigerator at ~3°C for 30 minutes. Both sides of the membrane were exposed to all surface treatments save the last. Instead, one solution well was filled with the reductant, formaldehyde, and the other side with the remaining components of the (formaldehyde-free) gold plating bath (Figure 2). Gold plating (that is, reduction of solution-phase Au(I) onto the surface as Au) was expected only where diffusion of both components of the divided Au(I) plating solution through the nanopore array generated sufficient concentrations of both partial solutions. Figure 2 shows scanning electron micrographs (SEM) and energy-dispersive x-ray spectroscopy (EDS) maps of the resulting metal deposition. The densest metallization was localized around the nanopore array locations. The length of the sides of each array was ~500 nm so that each occupied a small area within a noticeably metallized circle. The build-up of Sn and Ag at the edges where the unsupported SiNx membrane joins the Si-supported membrane is consistent with incomplete removal of plating solution during rinsing. This feature is not prominent in the Au map, most likely because its distance from the nanopores limits the available Au(I) plating solution concentration there for the 30 minute plating time. In contrast, the buildup of Au near the nanopore array was appreciable, and on the length scale of the image after the 30 minute plating time, the square nanopore array is effectively a point source. With uniform exposure of the SiN_x membranes to the Sn(II)- and Ag(I)-containing solutions, we had anticipated that only the gold plating step would reveal the nanopore array location, but the metals specific to each electroless plating bath were present at elevated levels on the surface surrounding the nanopore array. The throughmembrane nanopore array thus dramatically changes the usual electroless plating paradigm: instead of bulk solution access to the plating surface from one side, only, the array provided essentially back-side access through the membrane to compensate for any local transient depletion of the plating bath active species. Thus, mass transport of solution species through nanopores could be used in two ways: to localize solution delivery, and to provide an additional sample delivery path—using the nanochannels as vias—to a surface. Finally, the use of asymmetric electroless plating procedures allowed a direct microscopic illustration, at a fixed plating time, of the use of through-SiN_x-membrane nanochannels as an aperture for diffusional sample delivery that could be readily augmented with active sample delivery mechanisms such as voltage-induced fluid flow. The use of electroless plating in a nanopore, of course, transcends the view of nanopores as apertures, in that electroless plating was a vital tool in advancing nanopore single-molecule sensing. The approach allowed for size-tuning of polymer nanopores while simultaneously presenting a surface to create chemically decorated pores by thiol self-assembled monolayer formation. (25, 27-29)

In a similar confluence of nanoscale aperture and chemistry, a particularly interesting application of nanopores is in support of nanopore force spectroscopy (NFS).(30-34) Briefly, an analyte is driven into the pore with part of it too large to fit through, thereby applying a physical force—at the single molecule application and readout level—to explore such questions as the stability of molecular conformations and the energetics of intermolecular association. Nanopores are also fluid channels that conduct ionic currents which can be read out electronically, and thus nanopores provide a bridge between the world of electronics and ionics (e.g. Figure 1). As ionic circuit elements, nanopores can readily serve as resistors and rectifiers and offer resistance (or its inverse, conductance) that can be tuned by nanopore surface chemistry and by solution properties.(35-37)

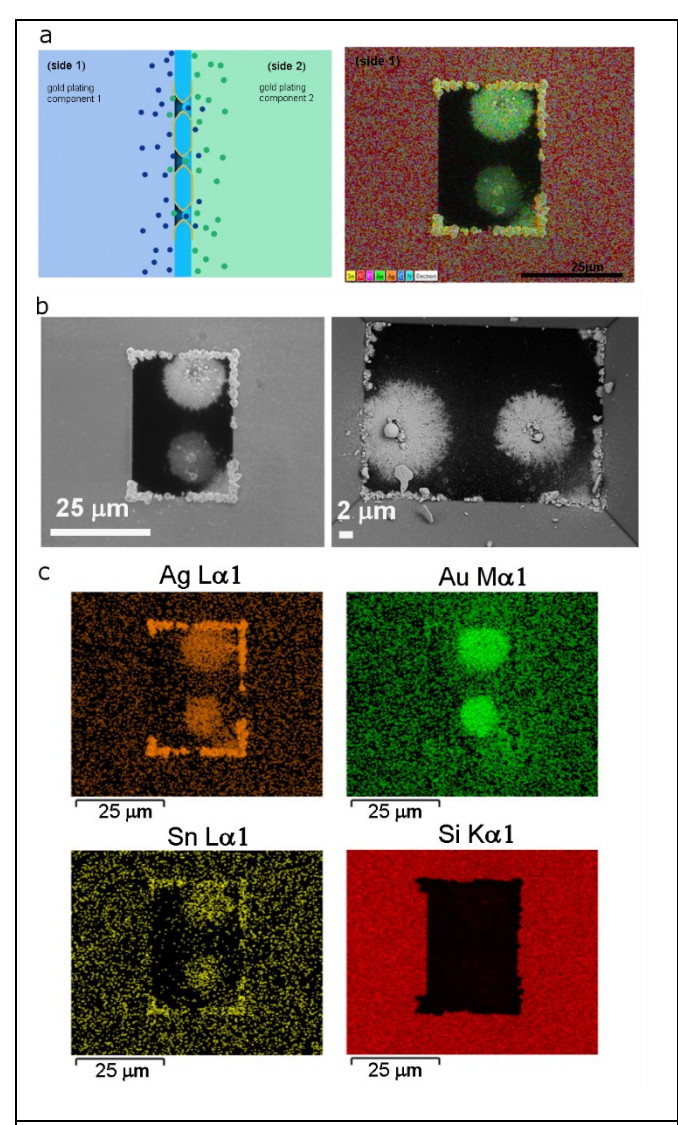


Figure 2. (a) Schematic illustrating the asymmetric configuration of the Au(I) plating bath with resulting EDS map showing metallization in the area of the nanopore array. All images are after all electroless

plating steps were completed. (b) Scanning electron micrographs of the two 5×5 nanopore arrays in a free-standing SiN_x membrane (center rectangle) supported on a silicon frame. The planar membrane side (formaldehyde) is shown at left; the etch pit side (remainder of Au plating solution) of the same membrane is shown at right. (c) Element-specific channels of the EDS map in (a) reveal the composition of the SEM features.

In nanopore-based endeavors (sensing and otherwise), the material composition of the nanopore is an important design parameter with a profound influence on achievable device architectures, capabilities, and performance. This manuscript focuses on silicon-rich silicon nitride (SiN_x).(16, 17) This material supports nanopores to be formed in free-standing, thin ~10 nm films, which can be favorable for sensing. SiN_x is also a conventional micro- and nanofabrication material, and thus promises greater ease and speed of commercial-scale-deployment of fundamental discoveries (Figure 1). By virtue of this fabrication compatibility, it can also be easier to integrate other single molecule sensing and manipulation capabilities into the same nanopore platform.(17) When the base material is inadequate for the desired nanopore application, or when additional control parameters are desired, surface chemistry may offer salvation.

Nanopore Surface Chemistry Basics. Nanopores can be described as nothing more than nanofluidic channels \leq 100 nm in length and \leq 100 nm in diameter formed through otherwise impervious membranes. Examination of the canonical protein nanopore, α -hemolysin, in Figure 3, puts paid to that spartan view. The pore is a highly reproducible self-assembling structure optimized by evolution with a native surface chemistry that draws upon the richness of properties inherent to the 20 naturally occurring amino acids. That richness can be expanded using tools of molecular biology coupled to the capability to insert other moieties such as cyclodextrin into the existing framework. In contrast to this, the canonical thin-film nanopore formed in SiN_x, has a much more limited native surface chemistry encompassing only Si, N, O, and H. This sort of solid-state pore is only a dull and dismal facsimile of its protein cousin when carbon-containing molecules are absent from its framework. Figure 3 provides an overview of this contrast between these two pore types, as well as an indication of how synthetic chemistry applied to solid-state pore design could be used to bridge the gap. With the availability of suitable surface functionalization methods, a wide range of organic films could be installed on the nanopore surface, even allowing the coupling of biomolecules.

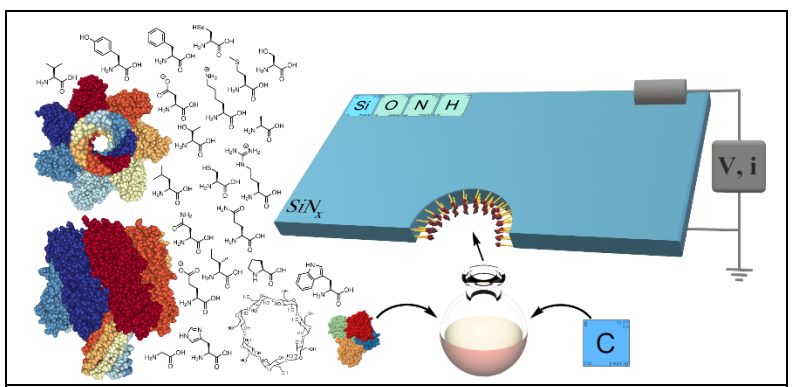


Figure 3. A protein nanopore, such as α -hemolysin(38) at left, can have complex surface chemistry owing to the variety of amino acid properties as well as the insertion of molecules such as cyclodextrin by standard protein modification methods. Thin-film silicon nitride pores at right have much simpler native surface chemistry. Surface chemical modification routes that unleash the potential of synthetic chemistry and support biofunctionalization can begin to blur the difference between the pore types. Molecular layers can be used to tune both the surface chemistry and the physical dimensions of the pore.

Over the years there have been demonstrations of approaches to increase the chemical complexity of nanopore interiors.(25, 36, 39-44) SiN_x nanopores have been an especially challenging target. Conventional silane chemistry has been used to functionalize the oxide coating that forms on SiN_x with organic monolayers.(41) The infrequency of adoption of this method underscores the difficulties that often plague the implementation of silane chemistry, and that are only exacerbated by the often spotty quality of the oxide coating (17) A fundamentally different, bioinspired approach—and one that also appears in capillary electrophoresis—involved flowing a lipid bilayer over the nanopore surface. (40) The translocating molecule is then faced with a fluid nanopore surface layer rather than the solid-state interface of the native, unfunctionalized SiN_x pore. We were interested in the benefits of covalent coupling to the nanopore surface and being able to use low-cost, robust, and generic molecules to coat the nanopore interior. At the same time we wanted to allow for flexible surface chemistry that could support the insertion of customsynthesized species while still allowing for the beneficial possibilities emerging from bioinspired coatings. Straightforward covalent attachment of organic species with terminal alkene groups to the excess silicon in SiN_x by photochemical or thermal hydrosilylation has been well-documented and developed, and shown capable of also enabling surface biofunctionalization.(45, 46) With the discovery of crucial steps for nanopore compatibility (replacement of hydrofluoric acid etching with controlled dielectric breakdown), we were able to successfully transfer this robust chemistry to the nanopore milieu (Figure 4).(36) The installation of nanopore surface coatings—with molecular-level control over layer thickness and terminal surface groups—allows nanometer-level control over nanopore dimension and chemical control over

passive nanopore characteristics. It can also play a vital role in the action of sensing, as will be outlined in later sections in the context of (1) nanopore transport and (2) nanopore carbohydrate analysis.

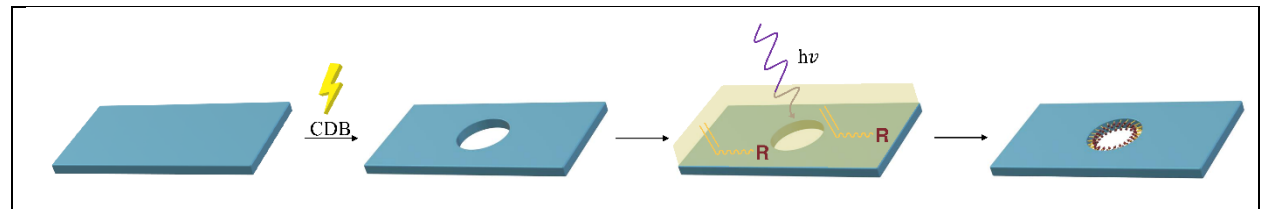


Figure 4: SiN_x nanopore surface functionalization by photohydrosilylation. Controlled dielectric breakdown is used to simultaneously form a nanopore in a thin SiN_x film and prepare its surface. This second, simultaneous function replaces a hydrofluoric acid chemical etching step that would increase the pore size. The as-formed pore is immersed in an alkene-terminated liquid and photoirradiated to form a monolayer-coated pore.(36)

Nanopore diameter can be estimated, using a cylindrical shape, from equation (1)

$$G = K \left(\frac{1}{\frac{\pi r_0^2 + \mu |\sigma|}{L} \cdot \frac{2\pi r_0}{K}} + \frac{2}{\alpha \cdot 2r_0 + \beta \cdot \frac{\mu |\sigma|}{K}} \right)^{-1} = \left(\frac{1}{G_{\text{bulk}} + G_{\text{surface}}} + \frac{1}{G_{\text{access}}} \right)^{-1}$$
(1)

where G, K, L, r_0 , σ , μ , α and β are the ionic conductance, electrolyte conductivity, nanopore length, nanopore radius, nanopore surface charge density, surface counterion mobility, and model-dependent parameters (both set to 2) respectively.(47, 48) Changes in nanopore conductance can thus be used to infer changes in nanopore dimension (often neglecting considerations of nanopore surface charge), of nanopore surface chemistry, or of both. Figure 5 illustrates how changes in nanopore radius due to surface coating can change the nanopore conductance. More sophisticated diagnostics of the conductance—involving changes of salt concentration or solution pH, for example—can be used to perform a more complete characterization of the nanopore.(49)

While (photo)hydrosilylation has been used to establish a base layer for the subsequent biofunctionalization of SiN_x thin films, this foundational work was carried out on accessible and well-characterized planar surfaces.(45, 46) We thus wanted to test whether the principle would extend to the nanopore interior. A fresh nanopore was fabricated in a ~10 nm-thick SiN_x membrane by controlled dielectric breakdown in a 1 M potassium chloride (KCl) solution stabilized at pH 7.4 with 10 mM HEPES. The membrane was then rinsed with water and ethanol, placed in a custom reaction chamber with 60 μ L of neat 5-hexenoic acid and irradiated at 254 nm for 3 h as detailed in earlier work.(36) The newly carboxylic-acid-functionalized membrane was rinsed with ethanol and its conductance was measured in the 1 M KCl electrolyte before rinsing in ethanol. The pore was then immersed in an aqueous solution of 10 mM 1-(3-dimethylaminopropyl)-3-ethylcarbodiimide hydrochloride (EDC) and 20 mM N-hydroxysulfosuccinimide

(Sulfo-NHS) stabilized at pH 5.5 with 0.1 M 2-(N-morpholino)ethanesulfonic acid (MES) for 30 min to achieve an active ester. This was then transferred for overnight soaking in an aqueous solution of 1 mg/mL concanavalin A (con A) stabilized at pH 6.5 by 0.1 M MES. The concanavalin-A-functionalized membrane was then rinsed with ethanol and the conductance was measured using the 1 M KCl solution used for dielectric breakdown. Figure 5 outlines the basic reaction steps and shows the change in the nanopore conductance after each functionalization step. Reproducible good agreement between changes in nanopore conductance and the thicknesses of mono- and few-layer films of small molecules has been wellestablished.(36, 41). Given the 6.0 nm×7.0 nm×7.0 nm size of the protein,(50) and the ~19 nm diameter of the nanopore, complete protein monolayer coverage at a density and uniformity that would be seen on a planar film is improbable in the nanopore, and to accurately determine the disposition of the protein relative to the nanopore interior would require significant experimental effort. Indeed, earlier work that inspired this effort reported ostensibly anomalous diameter changes after functionalization of polymer nanopores. While a reasonable mechanistic hypothesis for this discrepancy was provided, the result nevertheless underscores the complexity of the biofunctionalization challenge. (50) Our focus is thus the feasibility of biofunctionalization of thin SiN_x nanopores, assessed through observation of any changes to the nanopore conductance and any effect on the nanopore response to a test analyte. Compared to the preliminary stages of the small-molecule-based nanopore photohydrosilylation development, greater variability in initial biofunctionalization results underscores the chemical, physical and even geometric complexity of the challenge. The example illustrated here should thus be considered promising but reinforces the necessity for a comprehensive development effort. The neutral carbohydrate mannan (M7504, Millipore-Sigma, St. Louis, MO) was used to assay the effect of the nanopore coatings. As-formed, carboxylic-acid-coated (deprotonated and thus negatively surface-charged in the electrolyte used for these experiments), and concanavalin-A-coated nanopores were used. The electrolyte pH was 7.4 in 10 mM HEPES buffer with additional 138 mM sodium chloride, 2 mM potassium chloride, 1 mM calcium chloride, and 1 mM manganese chloride. (50) The unfunctionalized SiN_x nanopores showed a rapid decline in conductance with even the first aliquot of mannan, whereas the carboxylic acid showed a much less dramatic response in spite of its ~6 nm smaller diameter (Figure 5). Intriguingly, these proof-of-principle experiments suggest that the protein may have offered a degree of protection against fouling of the nanopore in comparison to unfunctionalized SiN_x nanopores. The unique features of nanopore sensing means that the mechanism for such a possible protective effect, if enduring in the face of rigorous examination, could harness electrokinetic phenomena in addition to mechanisms available to conventional surface passivation approaches that use proteins (e.g. bovine serum albumin (BSA)). This is a not insignificant potential outcome when a nanopore can potentially be clogged by even a single molecule. More importantly, these

preliminary results are consistent with the successful covalent biofunctionalization of thin-film SiN_x nanopores after photohydrosilylation.

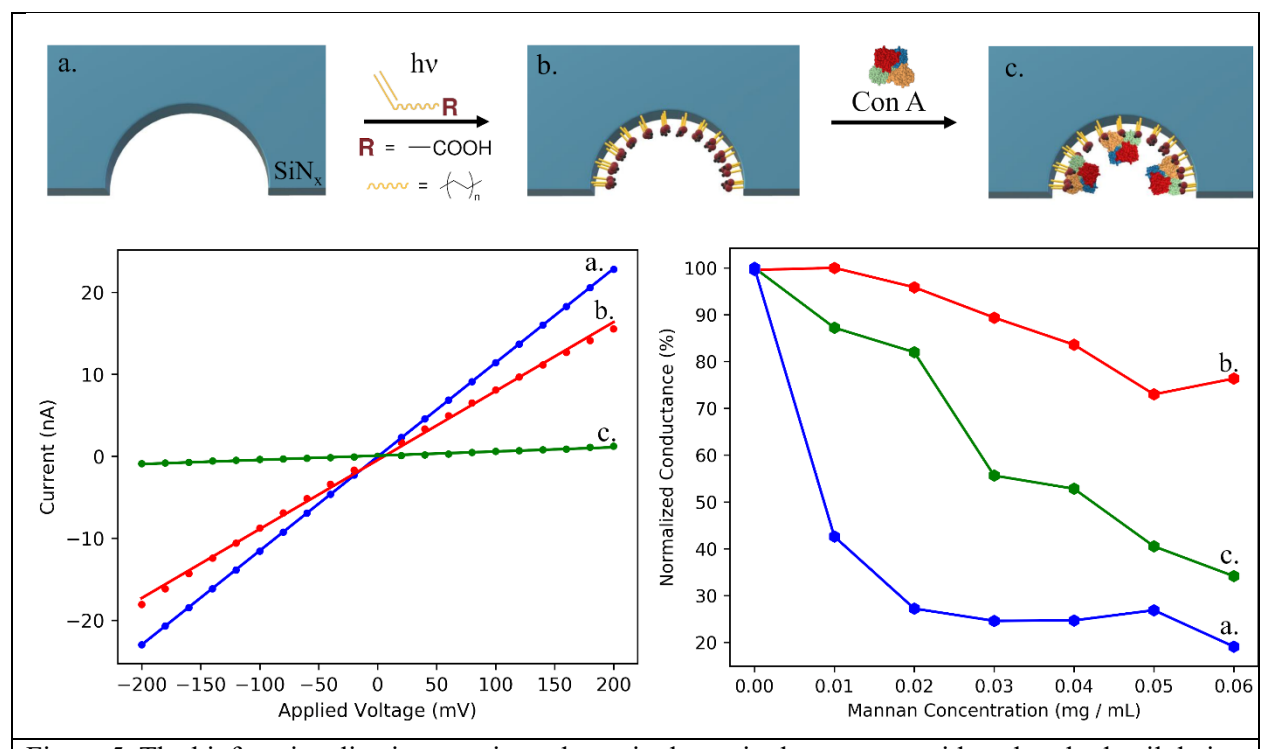


Figure 5. The biofunctionalization reaction scheme is shown in the top row, with a photohydrosilylation step followed by protein attachment. The change in nanopore conductance corresponding to each reaction step's change in the nanopore dimension can be determined from the current-voltage curves at lower left: from \sim 19 to 15 to 3 nm in diameter from (a) to (c). Further support for the success of each reaction step was shown by the changes in sensitivity of the different nanopores to increasing amounts of mannan. The results suggest that the protein may offer a degree of protection against fouling of the nanopore in comparison to unfunctionalized SiN_x nanopores. To prevent pore contamination affecting the results, the experiments were done using independent nanopores for (a) to (c) at lower right, with diameters \sim 18, 12, and 3 nm.

Chemical modification of the nanopore surface can affect much more than its conductance and propensity to (bio)foul. Quite sophisticated nanopore capabilities can spring forth with the installation of stimuli-responsive surface coatings, molecular recognition agents, and biomimetic coatings.(25, 39, 43, 44) Such powerful chemical transformations remain near the horizons of nanopore science, with much simpler transformations using conventional organic molecules still, themselves, offering largely untapped potential. Installing surface groups that participate in acid-base equilibria provide a simple means to control surface charges through both the chemical transformation step and the much simpler step of changing the solution pH. For the diprotic acid-base equilibria outlined in Table 1 and in Figure 6, there are distinct regions of pH where one of the forms of the species—either cationic, neutral, or anionic—dominates in aqueous solution (denoted by the fractional composition expression for each form i, α_i). A simple change of solution

pH changes which species will dominate. When the moiety A in Table 1 represents a surface-bound species, then a simple change of solution pH will change the dominant charge state of that surface. For a carboxylic-acid-terminated surface, for example, this change of protonation state can change not only the nanopore surface charge, but also its ability to chemically bind other species in solution. The protonation state and surface charge of nanopore (or analyte) surface at a particular pH will be determined by the particular values of the equilibrium constant(s) $\{K_a\}$.

Equilibrium	Equilibrium Constant	Fractional Composition
$H_2A^+ \rightleftharpoons HA + H^+$	$K_{a_1} \cong \frac{[H^+][HA]}{[H_2A^+]}$	$\alpha_{H_2A^+} = \frac{[H_2A^+]}{\Sigma} = \frac{[H^+]^2}{K}$
		$\alpha_{HA} = \frac{[HA]}{\Sigma} = \frac{K_{a_1}[H^+]}{K}$
$HA \rightleftharpoons A^- + H^+$	$K_{a_2} \cong \frac{[H^+][A^-]}{[HA]}$	$\alpha_{A^-} = \frac{[A^-]}{\Sigma} = \frac{K_{a_1} K_{a_2}}{K}$
	Where	$\Sigma = [H_2A^+] + [HA] + [A^-]$
		$K = [H^+]^2 + K_{a_1}[H^+] + K_{a_1}K_{a_2}$

Table 1. Chemical equilibria, acid dissociation constants, and fractional composition expressions for a diprotic acid H_2A^+ .

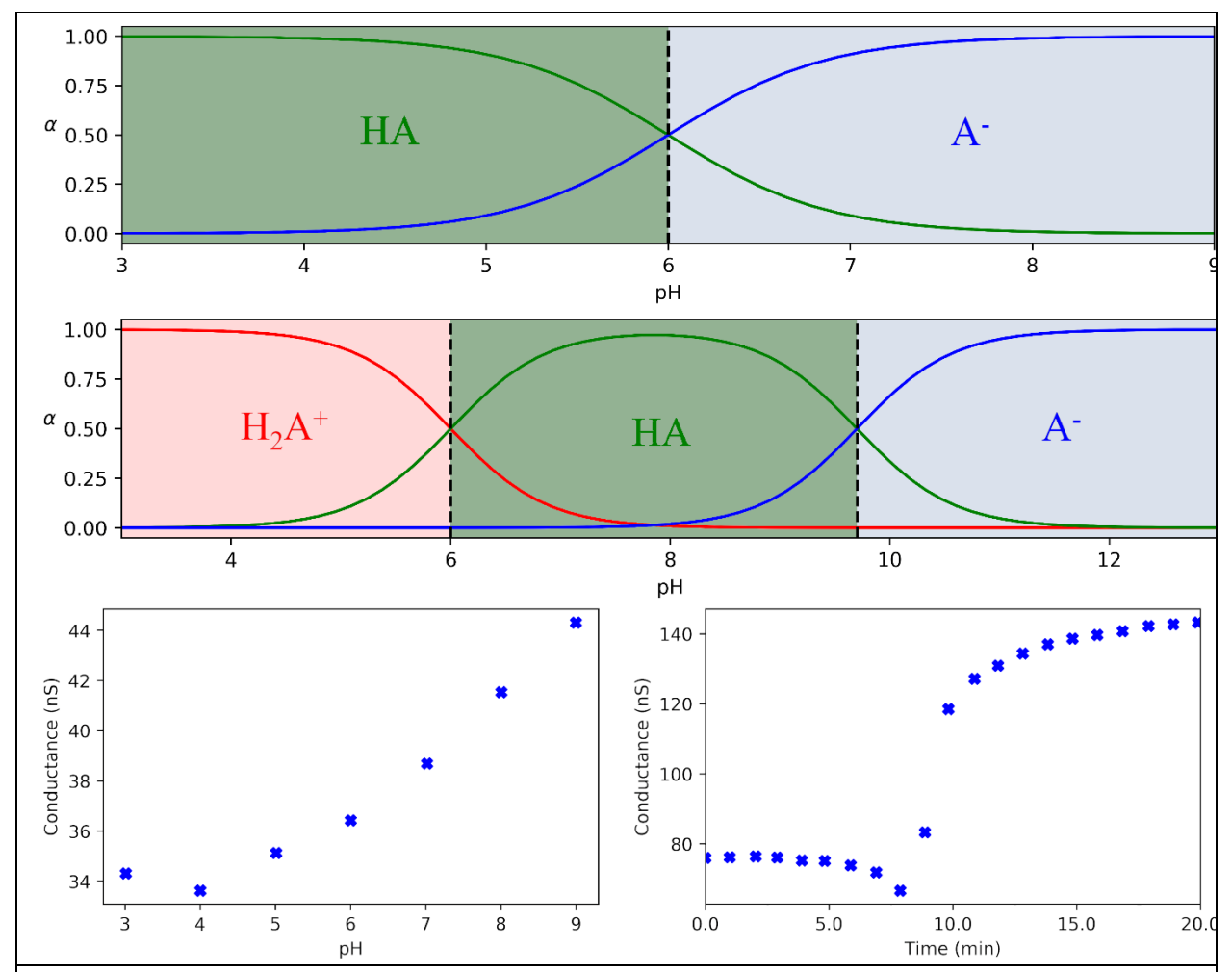


Figure 6. Fractional composition of a (top row) monoprotic and (middle row) diprotic acid, with $pK_a = 6$ and $pK_{a_1} = 6$, $pK_{a_2} = 9.7$, respectively. At bottom left, a plot of (~9 nm diameter) nanopore conductance versus solution pH for a diprotic surface neutral at pH~4 (see Equation 1 with $\sigma = 0$) and charged on either side of this minimum. At bottom right, a strong base was added to an acidic starting solution so that each time point corresponds to a different solution pH. For this ~13 nm diameter pore, an initially charged surface was rendered neutral after ~8 min (curve minimum) before becoming charged again. This approach essentially maps out the conductance versus (fixed) pH curve into conductance versus time.

The native surface chemistry of a SiN_x pore includes chemically available Si (as was necessary to support the photohydrosilylation reaction shown in Figure 4), hydroxyl (OH), and amine (NH₂) moieties.(17) In our earlier work we had successfully demonstrated a click reaction—a class of simple, quantitative, and byproduct-free reactions popular for coupling to biological molecules(51, 52)—after having initially installed an organic layer containing the NH₂-termination necessary to enable the coupling reaction. Indeed, one motivation of the development of the photohydrosilylation method was to have a single, general route to install monolayers with terminal groups that supported further chemical functionalization. The native surface chemistry of the SiN_x nanopore, however, offers different functional

groups for further reaction. While the actual composition and condition of the SiN_x surface can depend strongly on process history—one of the challenges facing silane chemical functionalization inside a nanopore(17)—controlled dielectric breakdown has been shown to be a powerful surface preparation treatment.(36) In Figure 7 we show conductance changes consistent with successful execution of the click reaction directly on unfunctionalized SiN_x nanopores without delay after formation by controlled dielectric breakdown. The IV curves indicate an ~8 nm diameter change accompanying the surface functionalization step. The plot of G versus pH is flat, showing an absence of pH-responsive surface functionality. This result is different from the evident effect of pH on nanopore conductance displayed when performing click coupling to a nanopore surface earlier terminated with an organic amine.(36) It is not against chemical intuition, however, and might arise from the differences in e.g. linker, between the two different click reaction implementations. Regardless of terminal group or linker type, the ability to chemically tune nanopore surface chemistry can have profound consequences for nanopore sensing and offers the unique capability to tune the conductance of this ionic circuit element with molecular-level control.

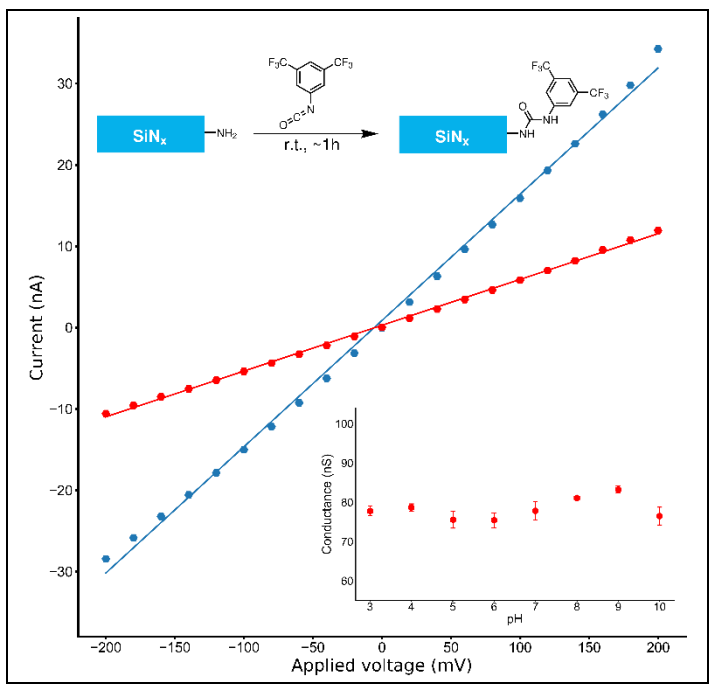


Figure 7. The terminal amine group on the native SiN_x surface is available for reaction, as shown in the click reaction here after CDB pore formation. The current-voltage plot shows the change in nanopore conductance from the as-formed pore (blue, ~23 nm diameter) to the coated pore (red, ~15 nm diameter). The inset shows the largely flat conductance vs. pH curve arising from the surface functionalization.

Nanopore Analyte Transport. One basic promise of nanopore sensing, albeit overly simplified, is that the nanopore sensor can detect every single molecule that passes through the pore. The trick is then to make sure that the molecules of interest make it to—and through—the nanopore in a reasonable amount of time (diffusion can deliver neutral analytes to the pore for detection, for example, but not necessarily quickly enough). The translocation time should not be so fast as to exceed electronic bandwidth limitations, nor should the time between passages be so long at a given concentration as to prevent enough single molecule events for good measurement statistics. Indeed both areas of analyte transport are the focus of considerable research effort spanning from simple changes of electrolyte chemistry to the use of sophisticated interventions on the nanoscale.(53-57) In this article we will focus on how chemical tuning of the nanopore surface can be used to powerfully augment analyte manipulation by the most prevalent method, electrophoresis. Just as Coulter Counting can provide a palpable entry point to the basic principle of nanopore sensing, core (electrokinetic) nanopore operational principles can be found in the more familiar domain of capillary electrophoresis. (58) While the typically ≤1 V applied voltages used in nanopore sensing are much smaller than the kV voltages used in capillary electrophoresis, with conductive electrolytes (e.g. 1 M KCl_(aq)) the most significant voltage drop is on the length scale of the \sim 10 nm-long pore, giving rise to electric fields of 108 V/m. Of course operation on the nanoscale can quickly require the introduction of additional new considerations beyond what is seen in capillary electrophoresis, and may eliminate others, but there are nevertheless useful conceptual overlaps for those already familiar with capillary electrophoresis.(59-62)

Charged molecules can be directly manipulated by an applied electric field, through electrophoresis, but uncharged molecules are not directly accessible to electrophoresis. Tuning the electrolyte composition to effectively charge neutral analytes—rendering them accessible to electrophoretic control by adsorption of charged species is feasible—but does not represent a simple, general approach to ensuring electrical control over analyte motion.(63, 64) Electroosmosis offers a general approach. This mechanism is operational in electrolyte-filled channels with charged walls: voltage-driven fluid flow through the channel will carry neutral species. The overall migration rate, v, in response to an applied electric field, E, is then given by

$$v = (\mu_{\rm ep} + \mu_{\rm eo})E \tag{1}$$

The electrophoretic mobility, μ_{ep} , is determined by the analyte size (through friction), and the *analyte* charge and polarity. In contrast, the electroosmotic mobility, μ_{eo} , is dictated by the *channel wall* charge and charge polarity. Electrophoresis and electroosmosis can thus be competitive or cooperative and can act independently in the absence of either analyte or channel wall charge. The ability to control nanopore

surface chemistry—thus charge magnitude and polarity—can therefore prove a powerful means to control analyte transport by tuning the balance between electrophoresis and electroosmosis.

Electrokinetic manipulation of analytes in nanopore sensing can be augmented by chemical transformation of the nanopore surface and by solution-control over the nanopore and analyte surface charges. When either of those two surfaces participates in an acid-base equilibrium, a change of solution pH can change the overall presence and polarity of the effective charge, as shown in Figure 6. An ostensibly undetectable neutral analyte in a neutral pore might become readily detectable by a simple change of solution pH if either the analyte or nanopore surface becomes charged by a change of overall protonation state. Figure 8 illustrates this effect for a neutral analyte (maltodextrin) being "sensed" using a nanopore that has a neutral surface over a wide useful pH range before becoming anionic at quite basic pH. This surface chemistry was established by a chemically-tuned controlled dielectric breakdown process, with sodium hypochlorite added to the electrolyte during the nanopore fabrications step. (65) There was, by this approach, no need for a post-fabrication step such as photohydrosilylation to subsequently adjust the asformed nanopore surface chemistry. The neutral maltodextrin is readily detected at sufficiently basic solution pH where there is a net charge on the nanopore surface and thus an electroosmotic driving force. With a less basic pH resulting in a net uncharged nanopore surface, and the absence of an electrophoretic driving force on the neutral analyte, there were no analyte detection events. Upon pressing on to a more acidic pH, however, the frequency of current blockages increased dramatically. No electroosmotic driving force was expected, nor was charging of the analyte to make electrophoresis operational. Instead, we suspect that the onset of events arose from acid hydrolysis of the maltodextrin to generate charged fragments. This hypothesis drives home a key benefit of controlled surface functionalization. A change of solution pH will simultaneously affect the surface charge of analyte (μ_{ep}) and nanopore (μ_{eo}) , and their native properties may not allow for optimal sensing performance at any pH. By suitable choice of nanopore surface terminal group (and thus pK_a) the pH at which electroosmosis can be turned on or off can be (1) set without regard for the underlying nanopore surface's native acid-base behavior; (2) set to avoid conditions unfavorable to an analyte; and (3) set to compensate for any acid-base behavior of the analyte, itself. In other words, the ability to tune nanopore surface chemistry allows one to decouple the electrokinetic mechanisms (electrophoresis or electroosmosis, or both) operational at a given solution pH from the native chemical properties of the analyte, itself.

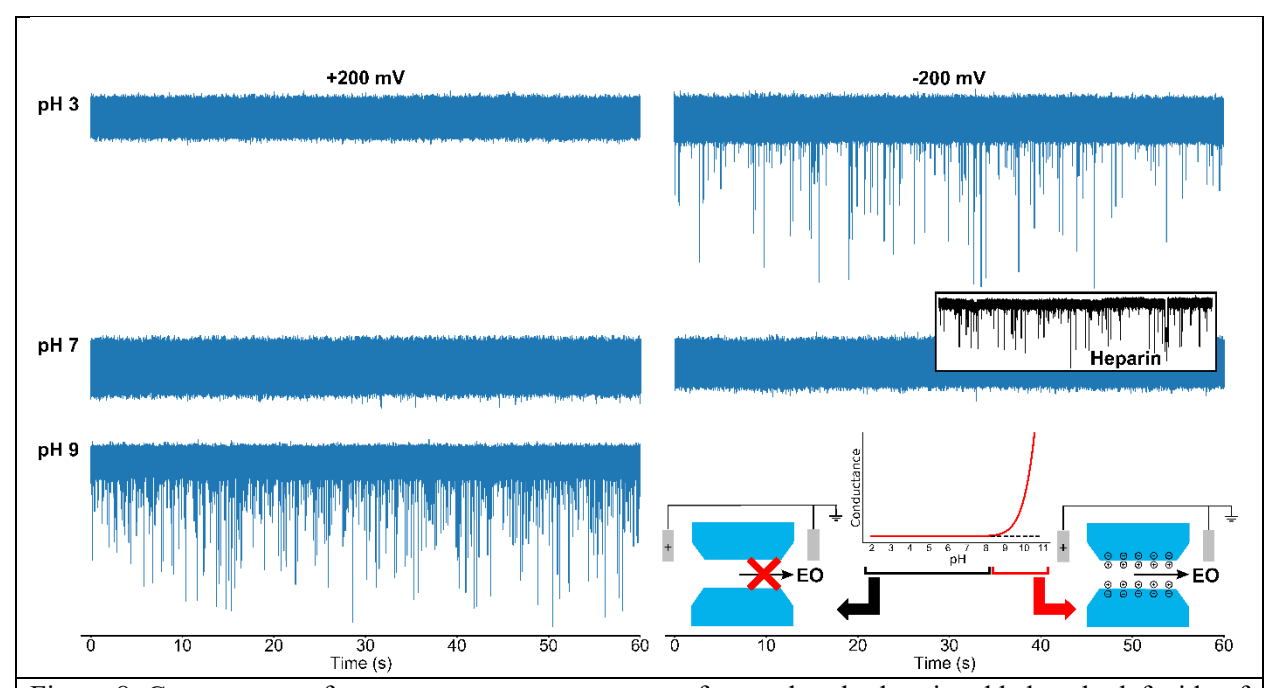


Figure 8. Current traces from nanopore measurements of neutral maltodextrin added to the left side of the pore in the image. At basic pH, the nanopore surface (~5 nm diameter) is charged and electroosmosis (EO) is active. Current blockages indicate that neutral maltodextrin is being detected. At neutral pH, the pore surface is uncharged and electroosmosis is no longer possible. At the same solution pH (using an independent ~5 nm-diameter pore with the same surface chemistry), however, anionic heparin is readily detected because it can be electrophoretically manipulated. At acidic pH, the pore surface remains uncharged but probable acid hydrolysis of the analyte leads to detectable events of charged fragments.

In nanopore sensing, molecules can be manipulated by electophoresis(60-62) and electrosmosis(7, 60-62, 66-69) in isolation or in tandem.(6) The information content of nanopore sensing can thus be dramatically enriched when a change of solution composition—as simple as its pH—is used as an added independent variable in nanopore assays. Through such a measurement paradigm, uncovering the number and magnitudes of an analyte's set of pK_a values, for example, can provide crucial chemical insights into an analyte's identity. Changes of electrolyte pH—and nanopore surface chemistry—can thus be used to enhance the selectivity of nanopore sensing. When evaluating the effect of changes of the electrolyte composition such as pH, however, it is important to realize that observed effects can be operational through electrostatics, changing specific chemical interactions, and through electrokinetics.

Nanopore Glycomics. The most high profile application of nanopore single molecule sensing—supported by extensive foundational research efforts—has been in the domain of genomics, for sequencing DNA (and RNA(70)).(30, 71, 72) Passage of this biopolymer through the nanopore sees the current perturbed for the entire passage time, with the transient current imprinted with the sequence of the bases trapped within the nanopore sensing zone at each instantaneous time point. DNA is anionic by virtue of its phosphate backbone and can thus be moved to and through the nanopore by virtue of electrophoresis. Nanopore protein analysis

is more complicated because of the variable biopolymer charge density arising from the variability in pK_a across the amino acids, and the prevalence of 1°, 2°, 3°, and 4° structures. (28-30, 61, 73-93) Depending on analyte and nanopore charge distributions, electroosmosis could dominate electrophoresis as the mechanism by which the protein is translocated through the nanopore, and this could well change along the length of the molecule. (62, 66) Whether electrophoresis or electroosmosis will dominate can be modulated, as outlined earlier, by solution pH and nanopore surface chemistry. It is perhaps the prevalence of DNA studies and corresponding easy reliance on electrophoresis in nanopore science that resulted in electroosmotic travel of a protein opposite to the electrophoretic direction being described as "anomalous" translocation behavior' (62) In nanopore sensing of DNA and proteins, nanopore size can be set so that only passage of the unfolded, linear conformation of the biopolymers is possible (with unfolding processes a possible target of study). In sequencing these linear, single-stranded biopolymers, an instantaneous current perturbation must be assigned to one of 4 possible simple monomers for DNA (increasing only slightly when considering DNA methylation of importance for epigenetics), or one of the 20 possible naturally occurring amino acids for proteins. In contrast to the genomics and proteomics cases, carbohydrate analysis is considerably more daunting. (9, 10) At the basic level of analyte manipulation, many of the carbohydrate oligomers and polymers are neutral even after reasonable changes of solution pH, thus eliminating the appealing control mechanism of electrophoresis. At the level of sequencing, the increased chemical complexity of the carbohydrates is clear: an instantaneous current level must be assigned to one of 120 naturally occurring monomers in correct order; with identification of the linkage types between monomers (fixed in the other two biopolymer examples); and polymer branching must also be contended with. (7, 10) Figure 9 illustrates this profound increase in complexity when comparing carbohydrate analysis to that of the other two canonical biopolymers.

Given the complexity of carbohydrate structure, and the challenges faced by even well-established conventional analysis tools, (9, 10) our approach to nanopore glycomics encompasses several different perspectives. (6, 7) We draw upon a small but exciting body of existing work: these founding nanopore-based carbohydrate studies have touched on fundamental measurements of transport kinetics, tests of differentiation between $1 \rightarrow 4$ and $1 \rightarrow 6$ glycosidic bonds, monitoring of enzymatic digestion products, molecular-weight discrimination, analysis of multicomponent samples, and signal analysis. While few in number, these studies nevertheless provide a starting point for examining our perspectives on nanopore glycomics. (7, 8, 94-106) On the first level, the breadth of monomer and (branched) oligo- and polymer structures and properties means that there is inherent merit in performing survey studies to uncover potential difficulties, discover unexpected and favorable outcomes, and explore fundamental nanopore sensing mechanisms with a compelling new class of molecule. On the next level, these survey studies will begin to provide insights into the ability of the resistive-pulse nanopore method—including testing enhancements

such as chemical optimizations—to transduce unique carbohydrate sequences and structures into differentiable signals. At the least, signal differences may be able to identify carbohydrate classes, identify or map branching, determine polymer length, or supply a fingerprint useful for quality assurance purposes. A much more challenging level of exploration is in pursuit of carbohydrate sequence: monomer sequence, linkage type, and location of any branches. These levels of glycan analysis are outlined in the context of the assay of the prevalent clinical anticoagulant heparin presented in Figure 10.(7)

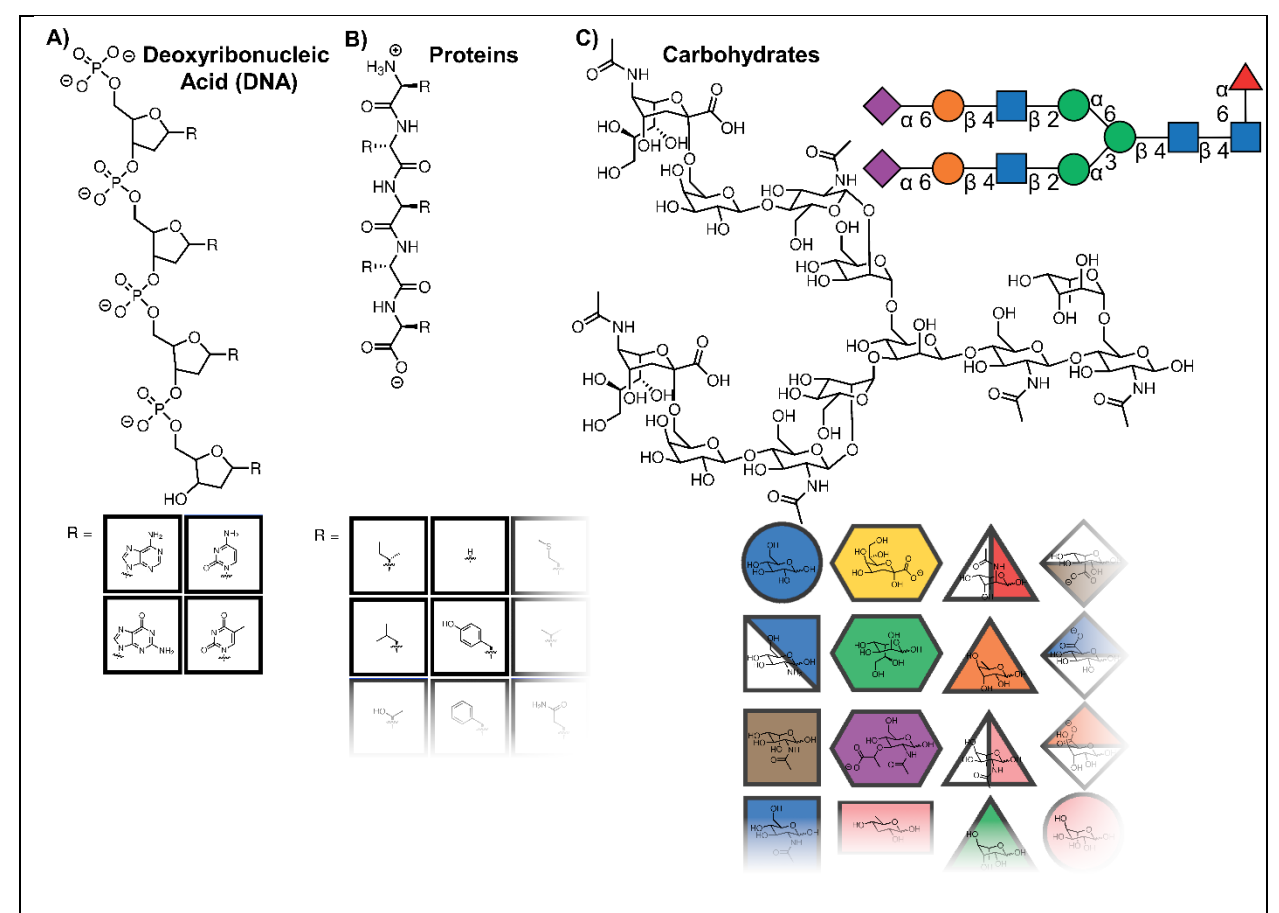
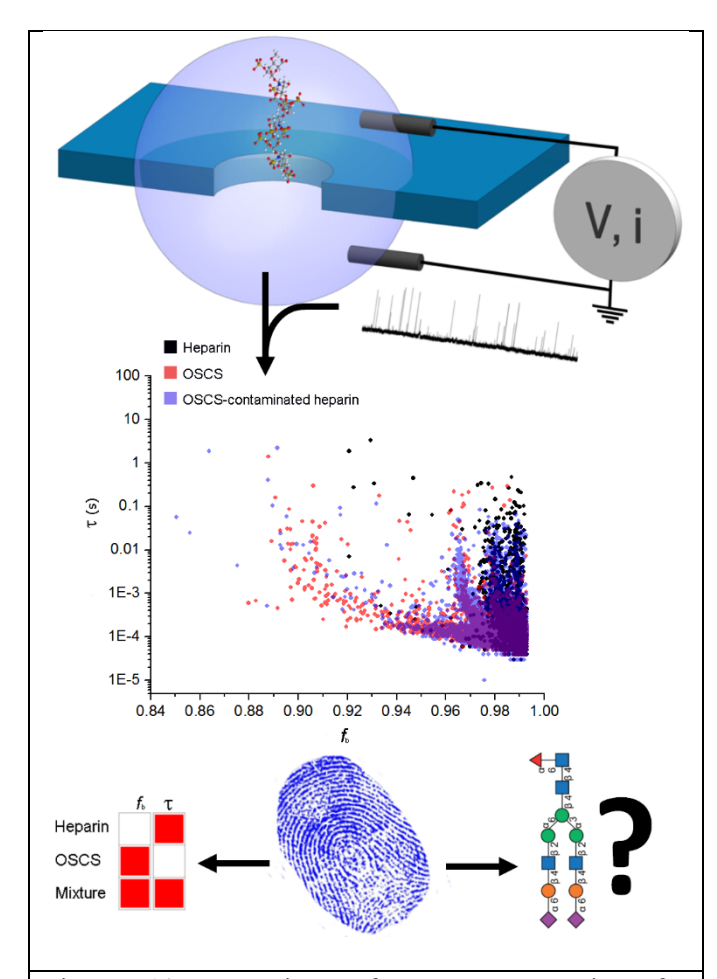


Figure 9. DNA and protein biopolymer 1° structure is determined by the sequence of 4 and 20 unique monomers (a subset of the 20 is shown). The polymers are linear and although proteins may adopt higher-order conformations, they can be linearized by a suitably sized nanopore. In contrast, carbohydrate oligo-and polymers consist of sequences of 120 possible monomers (a subset is shown) connected by different linkage types and with the possibility of branching. This chemical complexity is reflected in the adoption of drawing conventions to simply and quickly summarize the diversity of information needed for carbohydrate analysis. Such a compact representation is shown at the upper right.

In 2008, the clinical heparin supply was contaminated by a structurally similar adulterant, oversulfated chondroitin sulfate (OSCS), undetected by the standard screening protocols.(107-110) Yet it was readily detected by the body: adverse clinical consequences were the result, with the most profound being ~100 deaths in the United States.(107-112) Beyond the analytical challenge, heparin is the most

highly negative charge-dense biological molecule known, and so also presents a material challenge to nanopore sensing. (113) In earlier work, we used thin-film SiN_x nanopores to investigate the potential of resistive pulse sensing to differentiate between therapeutic and toxin.(7) OSCS appeared to interact more strongly than heparin with the (unfunctionalized) pore, and its blockages showed a ~2-fold higher current noise. When the individual current blockages were isolated and their duration and mean fractional blockage magnitudes (f_b the ratio of average blocked and unblocked pore currents) were plotted, further differences in event characteristics emerged (Figure 10). Even using the crude metrics of blockage duration and mean fractional blockage magnitude—without analyzing the current fluctuations and without using solution pH as an added experimental parameter—the blockage duration-magnitude scatter plots showed analytespecific distributions. These scatter plots can be thought of as "fingerprints" of their respective analytes. On the one hand they can provide a visual, qualitative guide for identifying one analyte or another. In the context of quality assurance assays, deviation of the fingerprint from its known appearance can be used as strong evidence of the presence of an impurity (whether of known identity or not)—one detected with a single-molecule-sensitive detector element. Of course, the scatter-plot fingerprint—and the underlying unaveraged data—may contain more information than is readily apparent by eye. Using a simple statistical thresholding algorithm, we were able to generate recognition flags as shown in Figure 10, in which the presence of heparin was determined from the duration (τ) distribution, the presence of OSCS was determined from the distribution of f_b , and the presence of both therapeutic and toxin was indicated by both parameters simultaneously. Such a straightforward analysis, while effective here, was limited in sophistication compared to what is feasible using machine learning.(8) Pattern recognition, though, is but the point of the spear for the possible contribution of nanopores to glycomics. By combining careful foundational studies with sophisticated data analysis, it may be possible to provide insight into carbohydrate branching patterns or perhaps even the long-term target of carbohydrate sequence information. Compared to the development path of nanopore DNA sequencing, a lack of commercial availability of high-quality glycan standards with sequences to-order and of compelling alternative glycan sequencing platforms complicates these pursuits. Nevertheless, the field is painstakingly undertaking to reach the critical mass and breadth of studies necessary to support, as has been done for nanopore DNA sequencing, more thorough exploration of considerations such as algorithm development to assess and improve sequencing error rates, and advisable experimental and signal parameter space ranges.(114-119)



Overview of nanopore sensing glycomics. Passage of a carbohydrate in electrolyte solution through a nanopore will generate a series of measurable current perturbations determined—and tunable—by a variety of factors. Differences in key characteristics of these current blockages—here, the blockage magnitude, f_b , and blockage duration, τ —as a function of analyte identity (therapeutic heparin vs. toxin OSCS vs. a mixture of both) can provide analysis selectivity. On one level, unique characteristics can be useful as the fingerprint of an analyte or analyte mixture. Statistical analyses of such fingerprints can reduce the complexity to more clearly definitive determinations such as the recognition flags at lower left. The ultimate goal of nanopore glycomics is whether such fingerprints can yield sequence information, as at bottom right.

Conclusions

The very origin of a nanopore's utility—its small size—is also what causes the greatest challenges to its use and whence enticing prospects emerge. CDB has largely eliminated the barriers to nanopore

formation in thin films, allowing research and development efforts to now no longer suffer for want of the basic tool—a very small hole. Tuned nanopore surface chemistry figures prominently in improving nanopore capabilities with familiar analyte classes, and in expanding the analyte scope beyond the familiar to more challenging species. Photohydrosilylation has quite dramatically increased the ease with which surface coatings—organic and biological, alike—can be installed on the surface of popular thin-film SiN_x nanopores. We have demonstrated how a suitable choice of nanopore coating—independent of or in tandem with changes to solution conditions such as pH—can tune a basic nanopore property such as its conductance; a more nuanced characteristic such as susceptibility to fouling; and functional capabilities such as accessible electrokinetic mechanisms for analyte transport. We have also further expanded the palette of feasible chemical functionalization strategies to include a click reaction directly onto a just-CDB-formed SiN_x nanopore surface.

The field of nanopore science has advanced not only in the sophistication and diversity of the chemical species installed on the nanopore surface, but in the complexity and diversity of the analytes passing through the pore and past the surface. Nanopores have well-established prominence in genomics, are subject to ongoing development for proteomics, and their application to glycomics is in ascendance. Glycomics presents significant challenges to conventional chemical analysis, and this holds true for nanopore-based efforts, as well, although nanopores offer unique routes to possible advances. Only the charged subset of carbohydrates would be accessible to nanopore sensing if electrophoresis were the only means of controllably moving analytes. Electroosmosis—and the underlying role of nanopore surface chemistry—take on outsized influence when considering the likelihood of encountering uncharged carbohydrates. While the native acid-base chemistry of unmodified SiN_x nanopores provides the opportunity to tune the surface charge from positive to neutral and through to negative, the particular set of pK_as of their surface groups limits this to solution pH ranges that may not be compatible with analyte chemical stability. Thus, tuned nanopore surface chemistry is vital to the prospects of nanopore glycomics, and may prove vital in ensuring that a simple nanoscale hole can be used for insight ranging from molecular fingerprints to elucidation of sequence and structure. Taking a grander view of the role and influence of chemistry and materials science in nanopore science, improvements in the ability to fabricate nanopores has been—and will continue to be—advancing the field and range of capabilities both in terms of singlemolecule sensing across a range of analytes and in terms of the ancillary capabilities of nanoscale apertures. The promising results that have emerged from the ability to cope with carbohydrate chemical complexity foreshadow the use of nanopore sensors for more general sensing applications.

Acknowledgements

Funding

This work has been funded principally by National Science Foundation award CHE-1808344, in part by RI Research Alliance grants from the Rhode Island Science & Technology Advisory Council, and includes work supported by National Science Foundation CAREER award CBET-1150085.

We thank Julie C. Whelan for fabrication and measurements related to the electrolessly plated nanopore arrays in Figure 2.

Conflict of Interest / Compliance with Ethical Standards

Several authors have received patents for aspects of the surface chemistry modifications presented here.

References

- 1. Graham MD. The Coulter Principle: Foundation of an Industry. JALA: Journal of the Association for Laboratory Automation. 2003;8(6):72-81.
- 2. Kasianowicz JJ. Bio-inspired nanopore-based sensors: Comment on "Nanopores: A journey towards DNA sequencing" by M. Wanunu. Physics of Life Reviews. 2012;9(2):170-1.
- 3. Bandara YMNDY, Karawdeniya BI, Dwyer JR. Push-Button Method To Create Nanopores Using a Tesla-Coil Lighter. ACS Omega. 2019;4(1):226-30.
- 4. Waugh M, Briggs K, Gunn D, Gibeault M, King S, Ingram Q, et al. Solid-state nanopore fabrication by automated controlled breakdown. Nature Protocols. 2020;15(1):122-43.
- 5. Kwok H, Briggs K, Tabard-Cossa V. Nanopore Fabrication by Controlled Dielectric Breakdown. PLoS ONE. 2014;9(3):e92880.
- 6. Karawdeniya BI, Bandara YMNDY, Nichols JW, Chevalier RB, Hagan JT, Dwyer JR. Challenging Nanopores with Analyte Scope and Environment. Journal of Analysis and Testing. 2019;3(1):61-79.
- 7. Karawdeniya BI, Bandara YMNDY, Nichols JW, Chevalier RB, Dwyer JR. Surveying silicon nitride nanopores for glycomics and heparin quality assurance. Nat Commun. 2018;9(1):3278.
- 8. Im J, Lindsay S, Wang X, Zhang P. Single Molecule Identification and Quantification of Glycosaminoglycans Using Solid-State Nanopores. ACS Nano. 2019;13(6):6308-18.
- 9. National Research Council. Transforming Glycoscience: A Roadmap for the Future. Washington, DC: The National Academies Press; 2012. 208 p.
- 10. Czjzek M. Biochemistry: A wine-induced breakdown. Nature. 2017;544(7648):45-6.
- 11. Smeets RMM, Keyser UF, Krapf D, Wu M-Y, Dekker NH, Dekker C. Salt Dependence of Ion Transport and DNA Translocation through Solid-State Nanopores. Nano Lett. 2006;6(1):89-95.
- 12. Guo P, Martin CR, Zhao Y, Ge J, Zare RN. General Method for Producing Organic Nanoparticles Using Nanoporous Membranes. Nano Lett. 2010;10(6):2202-6.
- 13. Venta K, Wanunu M, Drndić M. Electrically Controlled Nanoparticle Synthesis inside Nanopores. Nano Lett. 2013;13(2):423-9.
- 14. Ierardi V, Becker U, Pantazis S, Firpo G, Valbusa U, Jousten K. Nano-holes as standard leak elements. Measurement. 2014;58:335-41.
- 15. Savard M, Dauphinais G, Gervais G. Hydrodynamics of Superfluid Helium in a Single Nanohole. Phys Rev Lett. 2011;107(25):254501.

- 16. Dwyer JR, Harb M. Through a Window, Brightly: A Review of Selected Nanofabricated Thin-Film Platforms for Spectroscopy, Imaging, and Detection. Appl Spectrosc. 2017;71(9):2051-75.
- 17. Dwyer JR, Bandara YMNDY, Whelan JC, Karawdeniya BI, Nichols JW. Silicon Nitride Thin Films for Nanofluidic Device Fabrication. In: Edel J, Ivanov A, Kim M, editors. Nanofluidics, 2nd Edition. RSC Nanoscience & Nanotechnology. 2 ed: Royal Society for Chemistry; 2016.
- 18. Striemer CC, Gaborski TR, McGrath JL, Fauchet PM. Charge- and size-based separation of macromolecules using ultrathin silicon membranes. Nature. 2007;445(7129):749-53.
- 19. Vlassiouk I, Apel PY, Dmitriev SN, Healy K, Siwy ZS. Versatile ultrathin nanoporous silicon nitride membranes. P Natl Acad Sci USA. 2009;106(50):21039-44.
- 20. Gironès M, Borneman Z, Lammertink RGH, Wessling M. The role of wetting on the water flux performance of microsieve membranes. Journal of Membrane Science. 2005;259(1–2):55-64.
- 21. Kuiper S, van Rijn CJM, Nijdam W, Elwenspoek MC. Development and applications of very high flux microfiltration membranes. Journal of Membrane Science. 1998;150(1):1-8.
- 22. Wang Y, Wang J, Gao M, Zhang X. A novel carbon material with nanopores prepared using a metal—organic framework as precursor for highly selective enrichment of N-linked glycans. Anal Bioanal Chem. 2017;409(2):431-8.
- 23. Yang J, Ferranti DC, Stern LA, Sanford CA, Huang J, Ren Z, et al. Rapid and precise scanning helium ion microscope milling of solid-state nanopores for biomolecule detection. Nanotechnology. 2011;22(28):285310.
- 24. Whelan JC, Karawdeniya BI, Bandara YMNDY, Velleco BD, Masterson CM, Dwyer JR. Electroless Plating of Thin Gold Films Directly onto Silicon Nitride Thin Films and into Micropores. ACS Appl Mater Interfaces. 2014;6(14):10952-7.
- 25. Sexton LT, Horne LP, Martin CR. Developing synthetic conical nanopores for biosensing applications. Molecular BioSystems. 2007;3(10):667-85.
- 26. Whelan JC, Karawdeniya BI, Bandara YMNDY, Velleco BD, Masterson CM, Dwyer JR. Correction to Electroless Plating of Thin Gold Films Directly onto Silicon Nitride Thin Films and into Micropores. ACS Appl Mater Interfaces. 2015;7(46):26004-.
- 27. Wharton JE, Jin P, Sexton LT, Horne LP, Sherrill SA, Mino WK, et al. A Method for Reproducibly Preparing Synthetic Nanopores for Resistive-Pulse Biosensors. Small. 2007;3(8):1424-30.
- 28. Sexton LT, Horne LP, Sherrill SA, Bishop GW, Baker LA, Martin CR. Resistive-Pulse Studies of Proteins and Protein/Antibody Complexes Using a Conical Nanotube Sensor. Journal of the American Chemical Society. 2007;129(43):13144-52.
- 29. Siwy Z, Trofin L, Kohli P, Baker LA, Trautmann C, Martin CR. Protein Biosensors Based on Biofunctionalized Conical Gold Nanotubes. Journal of the American Chemical Society. 2005;127(14):5000-1.
- 30. Reiner JE, Balijepalli A, Robertson JWF, Campbell J, Suehle J, Kasianowicz JJ. Disease Detection and Management via Single Nanopore-Based Sensors. Chem Rev. 2012;112(12):6431-51.
- 31. Tabard-Cossa V, Wiggin M, Trivedi D, Jetha NN, Dwyer JR, Marziali A. Single-Molecule Bonds Characterized by Solid-State Nanopore Force Spectroscopy. ACS Nano. 2009;3(10):3009-14.
- 32. Tropini C, Marziali A. Multi-nanopore force Spectroscopy for DNA analysis. Biophys J. 2007;92(5):1632-7.
- 33. Nakane J, Wiggin M, Marziali A. A nanosensor for transmembrane capture and identification of single nucleic acid molecules. Biophys J. 2004;87(1):615-21.
- 34. Mathe J, Visram H, Viasnoff V, Rabin Y, Meller A. Nanopore unzipping of individual DNA hairpin molecules. Biophys J. 2004;87(5):3205-12.
- 35. Guo W, Xia HW, Xia F, Hou X, Cao LX, Wang L, et al. Current Rectification in Temperature-Responsive Single Nanopores. Chemphyschem. 2010;11(4):859-64.
- 36. Bandara YMNDY, Karawdeniya BI, Hagan JT, Chevalier RB, Dwyer JR. Chemically Functionalizing Controlled Dielectric Breakdown Silicon Nitride Nanopores by Direct Photohydrosilylation. ACS Appl Mater Interfaces. 2019;11(33):30411-20.

- 37. Siwy ZS, Howorka S. Engineered voltage-responsive nanopores. Chem Soc Rev. 2010;39(3):1115-32.
- 38. Song L, Hobaugh MR, Shustak C, Cheley S, Bayley H, Gouaux JE. Structure of Staphylococcal α-Hemolysin, a Heptameric Transmembrane Pore. Science. 1996;274(5294):1859-65.
- 39. Eggenberger OM, Ying C, Mayer M. Surface coatings for solid-state nanopores. Nanoscale. 2019;11(42):19636-57.
- 40. Yusko EC, Johnson JM, Majd S, Prangkio P, Rollings RC, Li J, et al. Controlling protein translocation through nanopores with bio-inspired fluid walls. Nat Nanotechnol. 2011;6:253-60.
- 41. Wanunu M, Meller A. Chemically modified solid-state nanopores. Nano Lett. 2007;7(6):1580-5.
- 42. Sakai N, Matile S. Synthetic Ion Channels. Langmuir. 2013;29(29):9031-40.
- 43. Hou X, Guo W, Jiang L. Biomimetic smart nanopores and nanochannels. Chem Soc Rev. 2011;40(5):2385-401.
- 44. Lepoitevin M, Ma T, Bechelany M, Janot J-M, Balme S. Functionalization of single solid state nanopores to mimic biological ion channels: A review. Adv Colloid Interface Sci. 2017;250:195-213.
- 45. Arafat A, Giesbers M, Rosso M, Sudhölter EJR, Schroën K, White RG, et al. Covalent Biofunctionalization of Silicon Nitride Surfaces. Langmuir. 2007;23(11):6233-44.
- 46. Arafat A, Schroën K, de Smet LCPM, Sudhölter EJR, Zuilhof H. Tailor-Made Functionalization of Silicon Nitride Surfaces. Journal of the American Chemical Society. 2004;126(28):8600-1.
- 47. Detcheverry F, Bocquet L. Thermal Fluctuations in Nanofluidic Transport. Phys Rev Lett. 2012;109(2):024501.
- 48. Bandara YND, Karawdeniya BI, Dwyer JR. Push-Button Method To Create Nanopores Using a Tesla-Coil Lighter. ACS Omega. 2019;4(1):226-30.
- 49. Frament CM, Dwyer JR. Conductance-Based Determination of Solid-State Nanopore Size and Shape: An Exploration of Performance Limits. J Phys Chem C. 2012;116(44):23315-21.
- 50. Ali M, Ramirez P, Tahir MN, Mafe S, Siwy Z, Neumann R, et al. Biomolecular conjugation inside synthetic polymer nanopores via glycoprotein-lectin interactions. Nanoscale. 2011;3(4):1894-903.
- 51. Kolb HC, Finn MG, Sharpless KB. Click Chemistry: Diverse Chemical Function from a Few Good Reactions. Angewandte Chemie International Edition. 2001;40(11):2004-21.
- 52. Escorihuela J, Marcelis ATM, Zuilhof H. Metal-Free Click Chemistry Reactions on Surfaces. Advanced Materials Interfaces. 2015;2(13):1500135-n/a.
- 53. Wang Y, Yao F, Kang X-f. Tetramethylammonium-Filled Protein Nanopore for Single-Molecule Analysis. Anal Chem. 2015;87(19):9991-7.
- 54. Wanunu M, Morrison W, Rabin Y, Grosberg AY, Meller A. Electrostatic focusing of unlabelled DNA into nanoscale pores using a salt gradient. Nat Nano. 2010;5(2):160-5.
- 55. Lam MH, Briggs K, Kastritis K, Magill M, Madejski GR, McGrath JL, et al. Entropic Trapping of DNA with a Nanofiltered Nanopore. ACS Applied Nano Materials. 2019;2(8):4773-81.
- 56. Madejski GR, Briggs K, DesOrmeaux J-P, Miller JJ, Roussie JA, Tabard-Cossa V, et al. Monolithic Fabrication of NPN/SiNx Dual Membrane Cavity for Nanopore-Based DNA Sensing. Advanced Materials Interfaces. 2019;6(14):1900684.
- 57. Briggs K, Madejski G, Magill M, Kastritis K, de Haan HW, McGrath JL, et al. DNA Translocations through Nanopores under Nanoscale Preconfinement. Nano Lett. 2018;18(2):660-8.
- 58. Harris DC. Quantitative Chemical Analysis. 9 ed: W.H. Freeman and Company; 2016.
- 59. Faucher S, Aluru N, Bazant MZ, Blankschtein D, Brozena AH, Cumings J, et al. Critical Knowledge Gaps in Mass Transport through Single-Digit Nanopores: A Review and Perspective. J Phys Chem C. 2019;123(35):21309-26.
- 60. Schoch RB, Han J, Renaud P. Transport phenomena in nanofluidics. Reviews of Modern Physics. 2008;80(3):839-83.
- 61. Haywood DG, Saha-Shah A, Baker LA, Jacobson SC. Fundamental Studies of Nanofluidics: Nanopores, Nanochannels, and Nanopipets. Anal Chem. 2015;87(1):172-87.

- 62. Firnkes M, Pedone D, Knezevic J, Döblinger M, Rant U. Electrically Facilitated Translocations of Proteins through Silicon Nitride Nanopores: Conjoint and Competitive Action of Diffusion, Electrophoresis, and Electroosmosis. Nano Lett. 2010;6(8):895-909.
- 63. Robertson JWF, Rodrigues CG, Stanford VM, Rubinson KA, Krasilnikov OV, Kasianowicz JJ. Single-molecule mass spectrometry in solution using a solitary nanopore. P Natl Acad Sci USA. 2007;104(20):8207-11.
- 64. Reiner JE, Kasianowicz JJ, Nablo BJ, Robertson JWF. Theory for polymer analysis using nanopore-based single-molecule mass spectrometry. P Natl Acad Sci USA. 2010;107(27):12080-5.
- 65. Bandara YMNDY, Saharia J, Karawdeniya BI, Hagan JT, Dwyer JR, Kim MJ. Beyond Nanopore Sizing: Improving Solid-State Single-Molecule Sensing Performance, Lifetime, and Analyte Scope for Omics by Targeting Surface Chemistry During Fabrication. Nanotechnology. 2020 (accepted).
- 66. Anderson BN, Muthukumar M, Meller A. pH Tuning of DNA Translocation Time through Organically Functionalized Nanopores. ACS Nano. 2012;7(2):1408-14.
- 67. Weerakoon-Ratnayake KM, O'Neil CE, Uba FI, Soper SA. Thermoplastic nanofluidic devices for biomedical applications. Lab on a Chip. 2017;17(3):362-81.
- 68. Uba FI, Pullagurla SR, Sirasunthorn N, Wu J, Park S, Chantiwas R, et al. Surface charge, electroosmotic flow and DNA extension in chemically modified thermoplastic nanoslits and nanochannels. Analyst. 2015;140(1):113-26.
- 69. Haywood DG, Harms ZD, Jacobson SC. Electroosmotic Flow in Nanofluidic Channels. Anal Chem. 2014;86(22):11174-80.
- 70. Egatz-Gomez A, Wang C, Klacsmann F, Pan Z, Marczak S, Wang Y, et al. Future microfluidic and nanofluidic modular platforms for nucleic acid liquid biopsy in precision medicine. Biomicrofluidics. 2016;10(3):032902.
- 71. Branton D, Deamer DW, Marziali A, Bayley H, Benner SA, Butler T, et al. The potential and challenges of nanopore sequencing. Nat Biotechnol. 2008;26(10):1146-53.
- 72. Niedringhaus TP, Milanova D, Kerby MB, Snyder MP, Barron AE. Landscape of Next-Generation Sequencing Technologies. Anal Chem. 2011;83(12):4327-41.
- 73. Mathwig K, Albrecht T, Goluch ED, Rassaei L. Challenges of Biomolecular Detection at the Nanoscale: Nanopores and Microelectrodes. Anal Chem. 2015;87(11):5470-5.
- 74. Kudr J, Skalickova S, Nejdl L, Moulick A, Ruttkay–Nedecky B, Adam V, et al. Fabrication of solid-state nanopores and its perspectives. Electrophoresis. 2015;36(19):2367-79.
- 75. Harms ZD, Haywood DG, Kneller AR, Jacobson SC. Conductivity-based detection techniques in nanofluidic devices. Analyst. 2015;140(14):4779-91.
- 76. Taniguchi M. Selective Multidetection Using Nanopores. Anal Chem. 2015;87(1):188-99.
- 77. Miles BN, Ivanov AP, Wilson KA, Dogan F, Japrung D, Edel JB. Single Molecule Sensing with Solid-State Nanopores: Novel Materials, Methods, and Applications. Chem Soc Rev. 2013;42(1):15-28.
- 78. Howorka S, Siwy Z. Nanopore analytics: sensing of single molecules. Chem Soc Rev. 2009;38(8):2360-84.
- 79. Albrecht T, Edel JB, Winterhalter M. New developments in nanopore research—from fundamentals to applications. J Phys: Condens Matter. 2010;22(45):450301.
- 80. Freedman KJ, Haq SR, Edel JB, Jemth P, Kim MJ. Single molecule unfolding and stretching of protein domains inside a solid-state nanopore by electric field. Sci Rep. 2013;3.
- 81. Pastoriza-Gallego M, Breton M-F, Discala F, Auvray L, Betton J-M, Pelta J. Evidence of Unfolded Protein Translocation through a Protein Nanopore. ACS Nano. 2014;8(11):11350-60.
- 82. Payet L, Martinho M, Pastoriza-Gallego M, Betton J-M, Auvray L, Pelta J, et al. Thermal Unfolding of Proteins Probed at the Single Molecule Level Using Nanopores. Anal Chem. 2012;84(9):4071-6.
- 83. Merstorf C, Cressiot B, Pastoriza-Gallego M, Oukhaled A, Betton J-M, Auvray L, et al. Wild Type, Mutant Protein Unfolding and Phase Transition Detected by Single-Nanopore Recording. ACS Chem Biol. 2012;7(4):652-8.

- 84. Cressiot B, Oukhaled A, Patriarche G, Pastoriza-Gallego M, Betton J-M, Auvray L, et al. Protein Transport through a Narrow Solid-State Nanopore at High Voltage: Experiments and Theory. ACS Nano. 2012;6(7):6236-43.
- 85. Oukhaled A, Bacri L, Pastoriza-Gallego M, Betton J-M, Pelta J. Sensing Proteins through Nanopores: Fundamental to Applications. ACS Chem Biol. 2012;7(12):1935-49.
- 86. Singh PR, Bárcena-Uribarri I, Modi N, Kleinekathöfer U, Benz R, Winterhalter M, et al. Pulling Peptides across Nanochannels: Resolving Peptide Binding and Translocation through the Hetero-oligomeric Channel from Nocardia farcinica. ACS Nano. 2012;6(12):10699-707.
- 87. Jetha NN, Semenchenko V, Wishart DS, Cashman NR, Marziali A. Nanopore Analysis of Wild-Type and Mutant Prion Protein (PrP^C): Single Molecule Discrimination and PrP^C Kinetics. PLoS ONE. 2013;8(2):e54982.
- 88. Radu IS, Dhruti T, Andre M, Jeremy SL. Evidence that small proteins translocate through silicon nitride pores in a folded conformation. J Phys: Condens Matter. 2010;22(45):454133.
- 89. Shi W, Friedman AK, Baker LA. Nanopore Sensing. Anal Chem. 2017;89(1):157-88.
- 90. Yusko EC, Bruhn BR, Eggenberger OM, Houghtaling J, Rollings RC, Walsh NC, et al. Real-time shape approximation and fingerprinting of single proteins using a nanopore. Nat Nanotechnol. 2016;12:360.
- 91. Movileanu L, Schmittschmitt JP, Martin Scholtz J, Bayley H. Interactions of Peptides with a Protein Pore. Biophys J. 2005;89(2):1030-45.
- 92. Sha J, Si W, Xu B, Zhang S, Li K, Lin K, et al. Identification of Spherical and Nonspherical Proteins by a Solid-State Nanopore. Anal Chem. 2018;90(23):13826-31.
- 93. Restrepo-Pérez L, Joo C, Dekker C. Paving the way to single-molecule protein sequencing. Nat Nanotechnol. 2018;13(9):786-96.
- 94. Bacri L, Oukhaled A, Hémon E, Bassafoula FB, Auvray L, Daniel R. Discrimination of neutral oligosaccharides through a nanopore. Biochem Biophys Res Commun. 2011;412(4):561-4.
- 95. Fennouri A, Przybylski C, Pastoriza-Gallego M, Bacri L, Auvray L, Daniel R. Single Molecule Detection of Glycosaminoglycan Hyaluronic Acid Oligosaccharides and Depolymerization Enzyme Activity Using a Protein Nanopore. ACS Nano. 2012;6(11):9672-8.
- 96. Fennouri A, Daniel R, Pastoriza-Gallego M, Auvray L, Pelta J, Bacri L. Kinetics of Enzymatic Degradation of High Molecular Weight Polysaccharides through a Nanopore: Experiments and Data-Modeling. Anal Chem. 2013;85(18):8488-92.
- 97. Kullman L, Winterhalter M, Bezrukov SM. Transport of Maltodextrins through Maltoporin: A Single-Channel Study. Biophys J. 2002;82(2):803-12.
- 98. Zhao S, Zheng Y-B, Cai S-L, Weng Y-H, Cao S-H, Yang J-L, et al. Sugar-stimulated robust nanodevice: 4-Carboxyphenylboronic acid modified single glass conical nanopores. Electrochem Commun. 2013;36:71-4.
- 99. Zheng Y-B, Zhao S, Cao S-H, Cai S-L, Cai X-H, Li Y-Q. A temperature, pH and sugar triple-stimuli-responsive nanofluidic diode. Nanoscale. 2017;9(1):433-9.
- 100. Nguyen QH, Ali M, Neumann R, Ensinger W. Saccharide/glycoprotein recognition inside synthetic ion channels modified with boronic acid. Sensor Actuat B-Chem. 2012;162(1):216-22.
- 101. Vilozny B, Wollenberg AL, Actis P, Hwang D, Singaram B, Pourmand N. Carbohydrate-actuated nanofluidic diode: switchable current rectification in a nanopipette. Nanoscale. 2013;5(19):9214-21.
- 102. Sun Z, Han C, Wen L, Tian D, Li H, Jiang L. pH gated glucose responsive biomimetic single nanochannels. Chem Commun. 2012;48(27):3282-4.
- 103. Oukhaled G, Bacri L, Mathé J, Pelta J, Auvray L. Effect of screening on the transport of polyelectrolytes through nanopores. EPL (Europhysics Letters). 2008;82(4):48003.
- 104. Rivas F, Zahid OK, Reesink HL, Peal BT, Nixon AJ, DeAngelis PL, et al. Label-free analysis of physiological hyaluronan size distribution with a solid-state nanopore sensor. Nat Commun. 2018;9(1):1037.
- 105. Ma T, Balanzat E, Janot J-M, Balme S. Single conical track-etched nanopore for a free-label detection of OSCS contaminants in heparin. Biosens Bioelectron. 2019;137:207-12.

- 106. Li M, Xiong Y, Wang D, Liu Y, Na B, Qin H, et al. Biomimetic nanochannels for the discrimination of sialylated glycans via a tug-of-war between glycan binding and polymer shrinkage. Chemical Science. 2020;11(3):748-56.
- 107. Lester J, Chandler T, Gemene KL. Reversible Electrochemical Sensor for Detection of High-Charge Density Polyanion Contaminants in Heparin. Anal Chem. 2015;87(22):11537-43.
- 108. Kim D-H, Park YJ, Jung KH, Lee K-H. Ratiometric Detection of Nanomolar Concentrations of Heparin in Serum and Plasma Samples Using a Fluorescent Chemosensor Based on Peptides. Anal Chem. 2014;86(13):6580-6.
- 109. Liu H, Zhang Z, Linhardt RJ. Lessons learned from the contamination of heparin. Nat Prod Rep. 2009;26(3):313-21.
- 110. Korir A, Larive C. Advances in the separation, sensitive detection, and characterization of heparin and heparan sulfate. Anal Bioanal Chem. 2009;393(1):155-69.
- 111. Kishimoto TK, Viswanathan K, Ganguly T, Elankumaran S, Smith S, Pelzer K, et al. Contaminated Heparin Associated with Adverse Clinical Events and Activation of the Contact System. New Engl J Med. 2008;358(23):2457-67.
- 112. Guerrini M, Beccati D, Shriver Z, Naggi A, Viswanathan K, Bisio A, et al. Oversulfated chondroitin sulfate is a contaminant in heparin associated with adverse clinical events. Nat Biotech. 2008;26(6):669-75.
- 113. Linhardt RJ. 2003 Claude S. Hudson Award Address in Carbohydrate Chemistry. Heparin: Structure and Activity. J Med Chem. 2003;46(13):2551-64.
- 114. Kono N, Arakawa K. Nanopore sequencing: Review of potential applications in functional genomics. Development, Growth & Differentiation. 2019;61(5):316-26.
- 115. Winters-Hilt S, Akeson M. Nanopore Cheminformatics. DNA and Cell Biology. 2004;23(10):675-83.
- 116. Winters-Hilt S, Vercoutere W, DeGuzman VS, Deamer D, Akeson M, Haussler D. Highly Accurate Classification of Watson-Crick Basepairs on Termini of Single DNA Molecules. Biophys J. 2003;84(2):967-76.
- 117. Noakes MT, Brinkerhoff H, Laszlo AH, Derrington IM, Langford KW, Mount JW, et al. Increasing the accuracy of nanopore DNA sequencing using a time-varying cross membrane voltage. Nat Biotechnol. 2019;37(6):651-6.
- 118. Rang FJ, Kloosterman WP, de Ridder J. From squiggle to basepair: computational approaches for improving nanopore sequencing read accuracy. Genome Biology. 2018;19(1):90.
- 119. Chien C-C, Shekar S, Niedzwiecki DJ, Shepard KL, Drndić M. Single-Stranded DNA Translocation Recordings through Solid-State Nanopores on Glass Chips at 10 MHz Measurement Bandwidth. ACS Nano. 2019;13(9):10545-54.